Kinetic Study of Manganese Association to Demetallized Concanavalin A†

Gerald M. Alter‡ and James A. Magnuson*

ABSTRACT: The saccharide binding properties of the mitogenic lectin concanavalin A are linked to the association of two metals, Mn^{2+} and Ca^{2+}. We have examined the binding properties of these metals with the specific purpose of looking for interactions between them. In a previous publication [Alter et al. (1977) *Biochemistry 16*, 4034] we reported that preincubation with Ca^{2+} of demetallized concanavalin A changes Mn^{2+} binding from a noncooperative to a cooperative process. In an extention of these studies, we now report that preincubation with Ca^{2+} of demetallized concanavalin A has a profound effect on the kinetics of Mn^{2+} binding. Using electron spin resonance and proton relaxation enhancement methods to examine both the time course of Mn^{2+} binding and changes in the environment of bound Mn, we have found that Ca^{2+} slows Mn^{2+} association relative to the rate in the absence of Ca^{2+}. Time courses obtained upon addition of Mn^{2+} to Ca^{2+}-preincubated, demetallized concanavalin A are consistent with a rate-determining step involving binding of Mn^{2+} to the second manganese site of a concanavalin A dimer. Further, the pH dependence of the association rate indicates that two groups with pK values of approximately 5.3 and 6.0 influence the rate of this metal's association. Activation parameters for the process at pH 5.1 and 6.45 are also reported. Results of this kinetic study are combined with the previously reported equilibrium studies to propose a scheme for Mn^{2+} binding to Ca^{2+}-preincubated concanavalin A in which the rate-limiting step for the association process is the binding of a second Mn^{2+} to concanavalin A dimers.

Concanavalin A[1] (Con A) is a mitogenic lectin extensively used in the study of cell surfaces (Bittiger & Schnebli, 1976; Lis & Sharon, 1973). Con A interacts with cells by binding specifically to sugar moieties with the D-arabinopyranoside configuration at its C-3, C-4, and C-6 positions (Goldstein et al., 1965, 1973). Kalb & Levitski (1968) demonstrated that one Ca^{2+} and one transition metal ion per 25 500 molecular weight subunit are linked to saccharide-binding activity of the protein. The metal ion sites have been identified in X-ray studies (Becker et al., 1975; Hardman & Ainsworth, 1972).

Metal ion requirements for saccharide binding have been examined extensively. Previous experiments suggested that the transition metal site S1 must be occupied before the Ca^{2+} site S2 can be filled (Shoham et al., 1973). A simplified view of the process by which metals activate Con A is that following transition-metal binding to S1 the Ca^{2+} site S2 is prepared. The binding of Ca^{2+} to S2 results in a conformational change which increases the number of protein ligands binding to the metal in site S1. . Sequential binding of Mn^{2+} and Ca^{2+}, followed by a conformational change in Con A, has been demonstrated by several experimental techniques including electron spin resonance (Nicolau et al., 1969; Reed & Cohn, 1970) and proton magnetic resonance studies (Meirovitch et al., 1974; Barber & Carver, 1975; Grimaldi & Sykes, 1975; Brown et al., 1977). Kinetic studies on metal association rates are in qualitative agreement with the metal ion binding process described above (Brown et al., 1977; Grimaldi & Sykes, 1975).

We recently demonstrated that in the presence of Ca^{2+} the Mn^{2+} binding was cooperative (Alter et al., 1977). The research described herein is a kinetic study of the rate processes involved in Mn^{2+} association with Con A preincubated with Ca^{2+}. ESR spectroscopy and proton relaxation rate enhancement studies were used to monitor Mn^{2+} binding. Rate laws and activation parameters for the pH range 5–7 were determined, and a model for the steps in Mn^{2+} association is presented.

Materials and Methods

Con A was prepared from jack bean meal as described by Agrawal & Goldstein (1967). Gel electrophoresis at pH 4.5 and 7.5 under nondissociating conditions gave single bands (Shephard & Gurley, 1966). Sodium dodecyl sulfate–polyacrylamide gels (Weber & Osborn, 1969) gave band patterns characteristic of Con A (Wang et al., 1971; Abe et al., 1971). Con A concentrations were determined spectrophotometrically at pH 5.2 using an absorbance, $A_{280nm}^{1\%,1cm}$, of 12.4 (Yariv et al., 1968). Activity was measured by glycogen precipitation assays (Poretz, 1968). Con A was demetallized by treatment of protein solutions with 0.1 N HCl to bring the pH to 1.2 (Kalb & Levitzki, 1968). After 30 min at room temperature, the protein solution was dialyzed against distilled water at 4 °C until the pH reached 5.5–6.0. Atomic absorption showed that the apo-Con A had less than 0.02 mol of Zn^{2+} or Mn^{2+} and less than 0.04 mol of Ca^{2+} per mol of Con A subunits. This Con A preparation was used in all metal binding experiments.

In time courses followed by ESR spectroscopy, solutions of apo-Con A or apo-Con A preincubated with Ca^{2+} for 30 min at the experimental temperature were mixed with manganese chloride solutions of the appropriate concentration. Mixing was carried out in a simple stopped-flow apparatus which delivered the resultant solution to an ESR cell. Prior to mixing, the reactant solutions were preincubated for at least 30 min in a constant temperature bath set at the desired temperature. The temperature of the sample delivery system and ESR cavity was controlled to ±1 °C with a stream of dry nitrogen. Varian E-3 and E-9 ESR spectrometers were used to monitor changes in the intensity of the low-field extremum of the $(H_2O)Mn^{2+}$

† From the Program in Biochemistry and Biophysics, Department of Chemistry, Washington State University, Pullman, Washington 99164. *Received April 21, 1978.* This research was supported in part by U.S. Public Health Service Grant CA 14496. Portions of this paper are derived from the thesis of G.M.A. presented in partial fulfillment of requirements for a Ph.D. degree, Washington State University (1975).

‡ Present address: Biological Chemistry Program, School of Medicine, Wright State University, Dayton, Ohio 45431.

[1] Abbreviations used: Con A, concanavalin A; apo-Con A, concanavalin A with no Ca^{2+} or transition metal ions; Con A_2, concanavalin A dimer; Con A_2–Mn, a concanavalin A dimer with Mn^{2+} bound to a single manganese binding site; ESR, electron spin resonance; NMR, nuclear magnetic resonance; PRR, proton relaxation rate; Mops, morpholinopropanesulfonate.

0006-2960/79/0418-0029$01.00/0

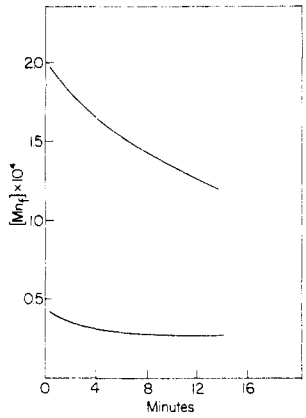

FIGURE 1: The effect of Ca^{2+} on the rate of binding of Mn^{2+} to apo-Con A preincubated with Ca^{2+}. Mn^{2+} concentration was followed by monitoring intensity of low-field extremum of ESR signal from free Mn^{2+}. For the lower trace Mn^{2+} was mixed with apo-Con A at time zero to give a solution 0.32 mM in Mn^{2+} and 0.34 mM in Con A monomers. For the upper trace apo-Con A was incubated with 6.0 mM Ca^{2+} for 30 min. At time zero this solution was mixed with Mn^{2+} and Ca^{2+} to give a 0.32 mM Mn^{2+}, 0.34 mM Con A monomer, and 6.0 mM Ca^{2+} solution. The pH was 6.5, and the temperature was 18 °C in the incubation and time courses.

ESR spectrum. The time resolution of the stopped-flow ESR apparatus was 1.0 s or less.

Water proton line widths were measured with a Varian A-60 NMR spectrometer equipped with a variable temperature probe. Reactant solutions were preincubated in the same manner as those used for ESR spectroscopy. The reactant solutions were mixed in an NMR tube and time-dependent changes in the spectrum of water protons were observed by repetitively taking continuous wave spectra of the water proton resonance after mixing. Enhancement values, ϵ^* (Dwek, 1973), were calculated from T_2 values which were determined from the water proton line width.

Solutions maintained at pH 5.5 or below contained 0.05 M acetate and 0.2 M NaCl. Solutions maintained above pH 5.5 contained 0.05 M Mops and 0.2 M NaCl. Buffer solutions were made with glass-distilled water and checked for Mn^{2+} and Ca^{2+} contamination by atomic absorption spectroscopy. All glassware was acid washed and thoroughly rinsed to avoid contamination by adventitious metals. In all kinetic experiments concentrations of reactants refer to concentrations after mixing at the beginning of each time course. Unless other units are specifically stated, concentrations of Con A are expressed in terms of 25 500-dalton Con A subunits.

Results

The time course of Mn^{2+} binding to Con A was readily monitored in stopped-flow ESR experiments. Isoclinic points have been observed in equilibrium titrations of apo-Con A with Mn^{2+} (Alter et al., 1977). Under the experimental conditions used, ESR spectroscopy monitored Mn^{2+} in only two states. The bound component contributes a relatively small paramagnetic resonance signal (von Goldhammer & Zorn, 1974; Alter et al., 1977) while the free Mn^{2+} signal is intense. At various times during a reaction time course the total Mn^{2+} spectra was composed of signals from free and bound Mn^{2+}. By following the intensity of the low-field maximum where the bound component makes a negligible contribution, the free Mn^{2+} concentration was monitored directly. The observed experimental result was a decrease with time in the Mn^{2+} signal as the cation bound to apo-Con A.

The rate for Mn^{2+} association to apo-Con A was profoundly affected by the presence of Ca^{2+}. In the pH range 5.0–7.0

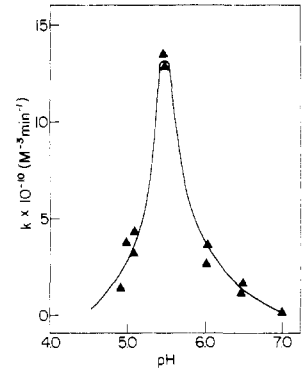

FIGURE 2: The pH dependence of rate constants k describing the rate of association of Mn^{2+} to demetallized Con A preincubated with an 8.5-fold excess of Ca^{2+} (with respect to Con A monomers) at 18 °C for 30 min. After mixing with Mn^{2+}, the solution was 3.0 mM in total Ca^{2+}, 0.35 mM in total Mn^{2+}, and 0.35 mM in total Con A monomers.

the rate of Mn^{2+} association to apo-Con A was faster than the time resolution of our apparatus (approximately 1.0 s). When apo-Con A was preincubated with Ca^{2+}, the rate of binding was markedly reduced and could be conveniently monitored by ESR spectroscopy (Figure 1). A similar time course was observed following incubation with half the Ca^{2+} concentration shown in Figure 1. All preincubations were carried out for 30 min, but a shorter period of 15 min did not alter the observed time course. The preincubation conditions used, therefore, appear to maximize the effect of Ca^{2+} in our experiments. All experiments reported here were conducted so as to maximize this effect. The rate of disappearance of the Mn^{2+} ESR signal was dependent on concentrations of both Mn^{2+} and Con A monomers. When initial concentrations of Mn^{2+} and Con A monomers were equal and Ca^{2+} was in large excess, the logarithm of the rate of the ESR signal change at any instant was a linear function of the logarithm of the Mn^{2+} concentration. The proportionality constant was four, indicating that with respect to Con A monomers and Mn^{2+} ions the total order for the observed reaction, the disappearance of free Mn^{2+}, was four (Laidler, 1965). Variation of initial concentrations of Mn^{2+} and Con A monomers in the presence of a 10-fold molar excess of Ca^{2+} indicated that the reaction was second order with respect to both Mn^{2+} and Con A monomers. The rate law describing the change in signal was given by eq 1, where Amp is the spectral amplitude, X is the

$$d[\mathrm{Amp}]/dt = k[Mn^{2+}]^2[\mathrm{Con\ A}]^2 = k[[Mn]_T - X]^2[[\mathrm{Con\ A}]_T - X]^2 \quad (1)$$

concentration of the metal–protein complex, and the subscript T indicates the total initial concentration of the particular reactant. The designation Con A represents a monomer with no associated manganese ion. Using the integrated form of the equation, time courses were analyzed with a nonlinear least-squares program and rate constants were calculated (Dye & Nicely, 1971). The precision of the fits was good, with estimates of uncertainties determined by this program of 1–5%. The time course of Mn^{2+} binding was examined over the pH range 5.0–7.0 with a 8.5-fold excess of Ca^{2+} with respect to Con A monomers. Equation 1 described all these time courses, and rate constants were determined. The pH dependence of the rate constants is summarized in Figure 2. A sharp maximum was observed at approximately pH 5.5, indicating that ionization states of at least two groups with relatively close pK values influence the rate of Mn^{2+} association with Con A. With a sixfold excess of Ca^{2+} similar rates were observed. With a fourfold excess a similarly shaped profile was observed,

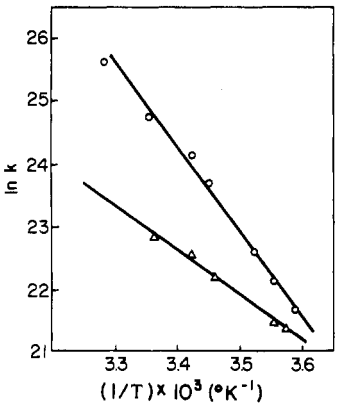

FIGURE 3: The temperature dependence of rate constants for the association of Mn^{2+} to Con A at pH 5.1 (O) and 6.45 (Δ). Rate constants were determined using reaction mixtures of apo-Con A which had been preincubated with an 8.5-fold excess of Ca^{2+} for 30 min at the experimental temperature. After mixing with Mn^{2+}, the final reaction mixture was 0.4 mM total Mn^{2+}, 0.47 mM in total Con A subunits, and 4.0 mM total Ca^{2+}.

Table I: Activation Parameters of Mn^{2+} Binding to Concanavalin A[a]

method	pH	$\Delta H^{\ddagger}$, kcal/mol	$\Delta S^{\ddagger}$, cal·deg^{-1}·mol^{-1}
ESR	5.1	27 ± 1.3[b]	80 ± 9[c]
ESR	6.45	14 ± 1.5[b]	34 ± 6[c]
PRR	5.1	29 ± 6[b]	75 ± 16[c,d]
PRR	6.45	14 ± 2.3[b]	25 ± 10[c,d]

[a] Expressed in terms of moles of Mn^{2+} bound. [b] Listed errors are the standard deviations of the slope of the fitted straight lines. [c] Listed uncertainties are derived from the uncertainties in $\Delta H^{\ddagger}$ and the standard deviation of rate constants from time courses followed at 16 °C. [d] Calculated using the calculated rate constant, Kk; see Results.

but it was shifted 0.4 pH unit to higher pH (data not shown). The temperature dependence of rate constants for Con A in the presence of an 8.5-fold excess of Ca^{2+} was determined at pH 5.1 and 6.5 and is shown in Figure 3. Activation parameters for the process calculated as described by Laidler (1965) are summarized in Table I.

While the ESR signal is virtually destroyed when Mn^{2+} binds to Con A, changes in water proton relaxation rates can reflect changes in the environment of Mn^{2+} after it is bound to the protein (Barber & Carver, 1973). Indeed earlier PRR studies by others showed that Ca^{2+} has a pronounced effect on the environment of the Mn^{2+} bound to Con A (Brown et al., 1977). We found that in all cases upon addition of Mn^{2+} to protein solutions the transverse proton relaxation rate enhancement, ϵ^* (Dwek, 1973), of water protons increased to values greater than 1.0 by the time of our first measurement (Figure 4). In the absence of Ca^{2+}, ϵ^* decreased very slowly and appeared to reach a constant value after 50 min at pH 5.0 and after 100 min at pH 7.0. The value of ϵ^* after these time periods was always greater than 1.0. Subsequent addition of a large excess of Ca^{2+} caused a rapid reduction of ϵ^* to values near zero by a process too fast for us to quantitate accurately. The rapid change appears to be exponential, which is consistent with the process being a Ca^{2+}-dependent conformational change as suggested by Brown & co-workers (1977). A typical time course for the rapid decrease of ϵ^* is shown in Figure 4. Initial values of ϵ^*, which were greater than 1.0 at all pH values and temperatures examined, indicated that water exchanged with at least one coordination position of Mn^{2+} bound to Con A in the presence and in the absence of Ca^{2+}.

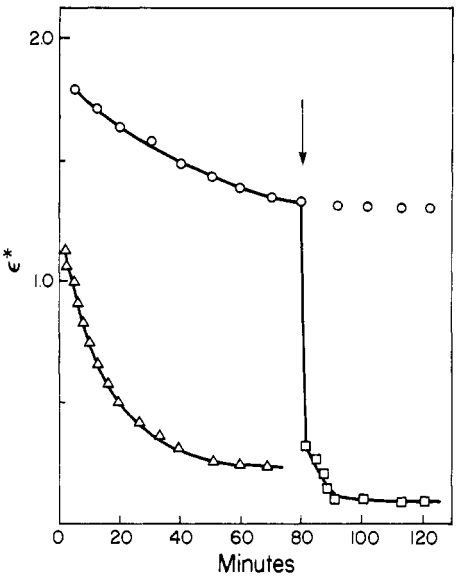

FIGURE 4: Time courses for proton relaxation rate enhancements, ϵ^*. The final concentration of Con A subunits was 0.33 mM. The concentration of all Mn^{2+} species present was 0.26 mM. Mn^{2+} was added to an apo-Con A solution which had been preincubated for 30 min with an 8.5-fold excess of Ca^{2+} (Δ). Mn^{2+} was added to apo-Con A not preincubated with Ca^{2+} (O); at the arrow a concentrated Ca^{2+} solution was added to produce an 8.5-fold excess of Ca^{2+} (□). The pH of the reaction mixture was 6.45 and the temperature was 28.5 °C.

Equal concentrations of Mn^{2+} and apo-Con A monomers, preincubated with Ca^{2+} as described earlier, were mixed and the time dependence of ϵ^* was followed. Total concentrations of Ca^{2+}, Mn^{2+}, and Con A monomer species were initially 3.0, 0.35, and 0.35 mM, respectively. When the results were analyzed for the overall order of the reaction by the same procedure used in the ESR experiments (Laidler, 1965), the order was found to be 2.0. A rate law consistent with this order is given by eq 2, where Con A_2–Mn represents a Con A dimer

$$d\epsilon^*/dt = k[\text{Con } A_2\text{–Mn}][Mn^{2+}] \quad (2)$$

(51 000 daltons) with one associated Mn^{2+}. The integrated form of the rate law is shown in eq 3, where t = i refers to

$$\frac{1}{[Mn^{2+}]_{t=i} - [\text{Con } A_2\text{–Mn}]_{t=i}} \times \ln \frac{[\text{Con } A_2\text{–Mn}]_{t=i}[Mn^{2+}]_t}{[\text{Con } A_2\text{–Mn}]_t[Mn^{2+}]_{t=i}} = F = kt \quad (3)$$

the time after an initial equilibrium between Mn^{2+} and Con A is established to form Con A_2–Mn. Because equilibrium is rapidly established, t = i is approximately the time of mixing. Concentrations at later times are indicated by the subscript t. Mn^{2+} and Con A_2–Mn contribute to ϵ^* and are extracted from observed values of ϵ^* during the time course using the relationship

$$\epsilon^* = \frac{[Mn^{2+}]_i - X}{[Mn]_T} + \epsilon^*_{Mn_B}\frac{[\text{Con } A_2\text{–Mn}]_i - X}{[Mn]_T} \quad (4)$$

The subscript i again refers to concentrations after equilibrium between Mn^{2+} and Con A is initially and rapidly established. The amount of Con A_2–Mn present during the reaction time course decreases by X. Con A_2–Mn is converted to the product Con A_2–Mn_2, a Con A dimer with two Mn^{2+} ions. The total Mn^{2+} concentration is represented by $[Mn]_T$ and $\epsilon^*_{Mn_B}$ is that ϵ^* characteristic of Con A_2–Mn. The justification for both the rate law and the analytical procedure is given in the Discussion.

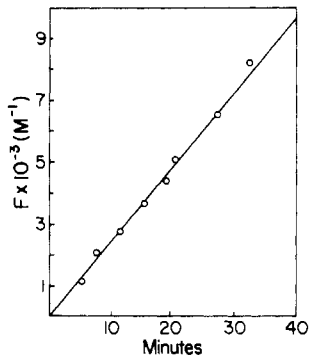

FIGURE 5: Representative analysis of proton relaxation data. Analysis was carried out according to eq 3 of the text where F is defined.

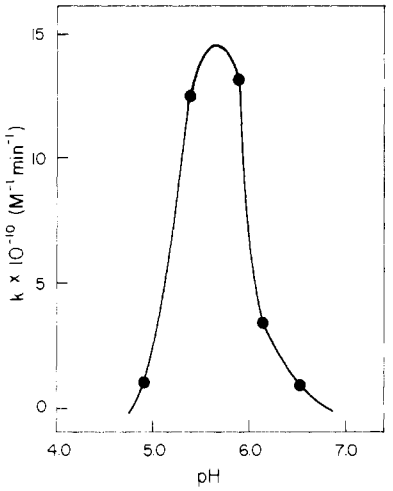

FIGURE 6: The pH dependence at 28.5 °C of rate constants k determined from PRR enhancement time courses following Mn^{2+} addition to apo-Con A preincubated for 30 min with Ca^{2+} in 8.5-fold excess with respect to Con A monomers. After mixing with Mn^{2+}, the solution was 3.0 mM in total Ca^{2+}, 0.35 mM in total Mn^{2+}, and 0.35 mM in total Con A monomers.

The time courses were well described by the integrated rate law, eq 3. When analyzed this way, the time course results gave linear plots with slopes equal to the rate constant for the process. A typical result is presented in Figure 5. The rate constants were pH dependent with a maximum near pH 5.5. The dependence is shown in Figure 6. As was found with the ESR studies, lowering the Ca^{2+} concentration would lead to a shift to higher pH values for the curve. As we did with the ESR studies, Ca^{2+} concentrations were chosen to be high enough to maximize the effect of Ca^{2+} and to give a pH profile at the lowest pH values.

The temperature dependence of PRR time courses was examined at pH 5.1 and 6.5. Linear Arrhenius plots were obtained at both pH values (Figure 7) and activation enthalpies determined (Table I). To facilitate the comparison of activation entropies characterizing ESR and PRR time courses, the rate law describing the PRR kinetic profiles was recast in terms of concentrations of Mn^{2+} and of Con A monomers. If the association of Mn^{2+} and Con A to form Con A_2–Mn (in the presence of Ca^{2+}) is characterized by the equilibrium constant K

$$[\text{Con } A_2\text{–Mn}] = K[\text{Con A}]^2[Mn^{2+}] \quad (5)$$

eq 2 can be rewritten as

$$\frac{d[\epsilon^*]}{dt} = kK[\text{Con A}]^2[Mn^{2+}]^2 \quad (6)$$

Thus, the rate constant in this formulation is the product of

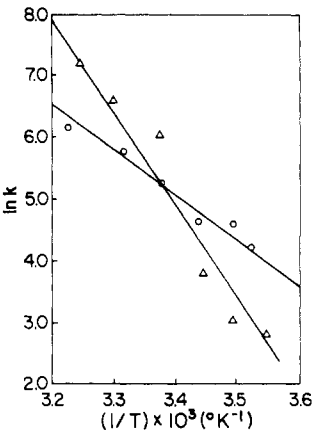

FIGURE 7: The temperature dependence of the rate constants for PRR time courses following Mn^{2+} addition to apo-Con A preincubated for 30 min at the experimental temperature with 9.5-fold excess Ca^{2+} with respect to Con A monomers at pH 6.45 (○) and pH 5.1 (△). After mixing with Mn^{2+}, the solution was 3.0 mM in total Ca^{2+}, 0.22 mM in total Mn^{2+}, and 0.32 mM in total Con A monomers.

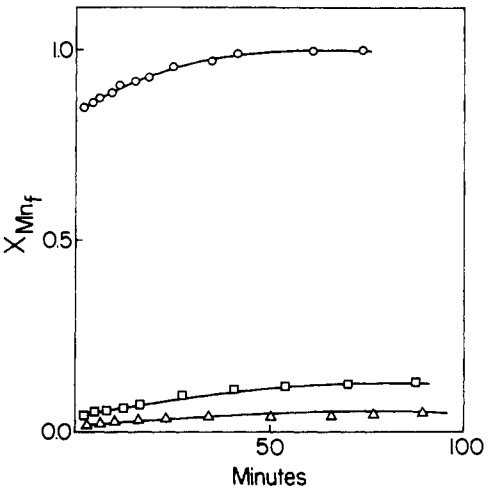

FIGURE 8: Time courses for the displacement of Mn^{2+} from Con A at 18 °C. The mole fraction of free Mn^{2+}, X_{Mn_F}, is plotted vs. time. Zn^{2+} was added at time zero to solutions of Con A (2.0×10^{-4} M in monomers) preincubated in 1.5×10^{-4} M Mn^{2+} (○); in 1.5×10^{-4} M Mn^{2+} and 2.0×10^{-3} M Ca^{2+} (□); in 1.5×10^{-4} M Mn^{2+}, 2.0×10^{-3} M Ca^{2+}, and 2.0×10^{-3} M methyl α-D-mannoside (△).

the rate constant in Figure 6 and the Mn^{2+} association constant which we have previously reported (Alter et al., 1977). By use of this new rate constant kK, entropies of activation were calculated. The results are summarized in Table I.

Finally, dissociation rates for Mn^{2+} bound to Con A in the absence and presence of Ca^{2+} and methyl α-D-mannoside were examined (Figure 8). The dissociation rate was measured by adding a 10-fold excess of Zn^{2+} and monitoring the free Mn^{2+} by ESR spectroscopy. Zn^{2+} binds more strongly than Mn^{2+} to Con A (Shoham et al., 1973) and would bind to any sites vacated by Mn^{2+}. The appearance of the Mn^{2+} ESR signal was, then, directly proportional to the amount of Mn^{2+} released from the Con A–manganese complex. The rate parameters for these processes were not determined since the extent of reaction observed was very small in all cases. The qualitative sense of the results, however, is clear; the rate of Mn^{2+} dissociation was drastically reduced in the presence of Ca^{2+} relative to the dissociation rate in its absence. In the presence of Ca^{2+}, the dissociation rate is so slow that, even after 100 min, only 10–15% of the Mn^{2+} was replaced by Zn^{2+}. Addition of a monosaccharide, methyl α-D-mannoside, further reduces the dissociation rate.

Discussion

In a recent communication we have reported that Mn^{2+} binding to Con A is modified by the presence of a second native metal Ca^{2+} (Alter et al., 1977). Although the stoichiometry of the reaction remains one Mn^{2+} per 25 500-dalton monomer regardless of the Ca^{2+} content, Mn^{2+} binding changes from a noncooperative process in the absence of Ca^{2+} to a cooperative process in the presence of an excess of Ca^{2+}. Here we report the consequences of Ca^{2+} preincubation on the rate of Mn^{2+} binding to Con A and its effect on the protein conformation in the vicinity of the metal binding areas. A mechanism for Mn^{2+} association is proposed below and is based on the results of both equilibrium and kinetic studies.

Rate Law for PRR Time Courses. The rate law for PRR time courses (eq 2) was deduced by determining both the total order of the reaction and the values of ϵ^* at the beginning of time courses. A mechanism where one Mn^{2+} and one Con A monomer bind in the rate-limiting step is consistent with the observed overall reaction order. For this mechanism the value ϵ^* would be proportional to the concentration of Mn^{2+} and the rate-limiting step would be followed by a rapid conformational change to an equilibrium state in which bound Mn^{2+} does not influence water proton relaxation. This mechanism, however, cannot be correct since it predicts that no PRR enhancement values greater than 1.0 would be observed. At the beginning of all time courses ϵ^* values were greater than 1.0 (for example, see Figure 4). Since ϵ^* for free Mn^{2+} is only 1.0 (Dwek, 1973), an intermediate consisting of Mn^{2+} bound to Con A must form before the initial PRR measurements are made. In addition this intermediate must have ϵ^* values greater than one. One possible intermediate is a Con A dimer with one Mn^{2+} bound so that water exchanges into and out of the first coordination sphere (Brown et al., 1977; Dwek, 1973). If the intermediate forms rapidly and nearly all Con A dimer is converted to the intermediate, the concentration of this intermediate and of free Mn^{2+} is approximately equal throughout each time course. The analytical procedure suggested by Laidler (1965), therefore, is valid. The observed second-order kinetics, based on the changes in ϵ^*, are consistent with the reactants being Con A_2–Mn and Mn^{2+}. A rapid conformational change could then mask both bound Mn^{2+} ions. The hypothesis is strongly supported by the ESR evidence which always showed that concentrations of Mn^{2+} equal to approximately half the concentration of Con A monomers were bound too rapidly to follow in our stopped-flow ESR experiments (Figure 1). Using values of equilibrium constants for the binding of the first Mn^{2+} to Con A dimers (Alter et al., 1977) and assuming that rapid binding occurs, we calculate that 90% or greater of all the Con A dimers in each time course had one metal bound at the time of our initial PRR measurement. It is a good approximation, therefore, that, under the experimental conditions used, the observed changes in PRR values arose from the reaction of Con A_2–Mn and Mn^{2+} to produce a Con A dimer with two bound Mn^{2+} ions. The initial concentrations of Mn^{2+} and Con A_2–Mn were routinely calculated assuming that rapid binding occurred. The concentrations of Mn^{2+} and Con A_2–Mn at later times are derived from the PRR enhancement at those times. Throughout the time course PRR enhancement values actually are the sum of contributions from Mn^{2+} in several environments as summarized by eq 7. The subscripts represent the

$$\epsilon^* = \epsilon^*_{Mn_f} X_{Mn_f} + \epsilon^*_{Mn_B} X_{Mn_B} + \epsilon^*_{Mn_{B'}} X_{Mn_{B'}} \qquad (7)$$

various environments: Mn_f, free Mn^{2+}; Mn_B, bound Mn^{2+} exchanging water; and $Mn_{B'}$, bound Mn^{2+} with slow or no water exchange. At equilibrium, $Mn_{B'}$ is the predominant environment. To determine Mn^{2+} and Con A_2–Mn concentrations throughout each time course, it is necessary to consider each contribution.

Koenig & co-workers (1973) examined the PRR properties of the complex represented by the $Mn_{B'}$ state. Using rotational correlation times, exchange lifetimes, and the number of exchanging water molecules reported by these authors, transverse proton relaxation times that characterize Mn^{2+} in this state were calculated as described by Connick & Fiat (1966). These calculations indicate that Mn^{2+} would contribute only about 0.2 Hz to the observed water proton line width. This value is no greater than experimental error and is consistent with a very small value of $\epsilon^*_{Mn_{B'}}$. The third term on the right-hand side of eq 7, therefore, can be eliminated. The value of $\epsilon^*_{Mn_f}$ is 1.0 so that eq 7 can be rewritten as

$$\epsilon^* = X_{Mn_f} + \epsilon^*_{Mn_B} X_{Mn_B} \qquad (8)$$

It is clear that ϵ^* directly measured in the experiment is partially dependent on the free as well as the bound manganese concentration. Rewriting eq 5 in molar quantities instead of mole fractions, one obtains eq 9, where the new terms represent

$$\epsilon^* = \frac{[Mn^{2+}]}{[Mn]_T} + \epsilon^*_{Mn_B} \frac{[\text{Con } A_2\text{–Mn}]}{[Mn]_T} \qquad (9)$$

the respective molar concentrations and the subscript T refers to total manganese. We assume that during the reaction free manganese Mn^{2+} is bound to Con A_2–Mn, so each binding produces the nonrelaxing species Con A_2–Mn_2 represented by $Mn_{B'}$. In each time course, free Mn^{2+} decreases by value X, Con A_2–Mn decreases by the same value, and $Mn_{B'}$ increases from zero to the value X. The appropriate equation derived from eq 9 is given by eq 4. The constant $\epsilon^*_{Mn_B}$ is determined using eq 8 and ϵ^* values obtained immediately after mixing reactant solutions.

Relationship between ESR and PRR Kinetics. The ESR and PRR studies provide different but related methods for monitoring Mn^{2+} binding. ESR time courses (Figure 1) essentially follow the disappearance of Mn^{2+} while PRR time courses (Figure 4) characterize interconversions between conformations of Con A–manganese complexes which are not detected in the ESR experiments. Initially Mn^{2+} bound to Con A must influence the water proton relaxation rate, since initial enhancement parameters greater than one were found in all PRR experiments. Decreases in relaxation enhancement to values approaching zero must arise from reorientation of the protein structure around the bound metal as the metal–protein complex attains its most stable conformation.

Our interpretation of PRR results focuses on a rearrangement of the protein's three-dimensional structure which in turn changes the water exchange properties of Mn^{2+}. This was originally suggested by Barber & Carver (1973). However, we cannot rule out alternative mechanisms in which subtle alterations in H_2O–Mn^{2+} bond energies account for decreases in PRR enhancements. The precise mechanism for PRR changes remains an open question.

The rate-limiting steps observed in both ESR and PRR studies are indistinguishable. The pH dependence of the rate constants for changes in proton relaxation rates (Figure 6) closely parallels the pH dependence of rate constants for disappearance of Mn^{2+} (Figure 2). Activation parameters summarized in Table I are the same for rate processes observed by both experimental techniques. Rate laws determined using both techniques (eq 1 and 2) are consistent with a rate-limiting step in which a second Mn^{2+} binds to a Con A dimer with one

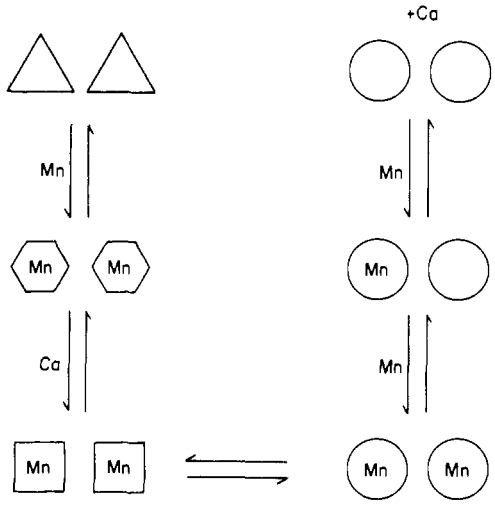

FIGURE 9: Scheme for addition of Mn^{2+} to Con A. Each pair of symbols represents a Con A dimer. Triangles are apo-Con A and circles are apo-Con A in the presence of Ca^{2+}. Addition of metal ion to a subunit is represented by placing the metal within the symbol. For details see Discussion.

Mn^{2+} site already occupied. We, of course, cannot prove on the basis of the kinetic data presented here that this is the only possible rate-limiting step.

Reaction Sequence for Mn^{2+} Binding to Con A. A sequence which is consistent with both the kinetic results reported here and equilibrium measurements previously reported (Alter et al., 1977) is schematically summarized in Figure 9. The intermediates in the association process have been identified using both PRR and ESR measurements. A pair of subunits or Con A dimer is represented by two identical symbols in this scheme. The triangles represent demetallized Con A. Binding of Mn^{2+} to a Con A subunit is represented by placing Mn^{2+} in the center of a symbol. Circles correspond to subunits preincubated with Ca^{2+} and in a conformational state that allows bulk water to exchange with the bound Mn^{2+}. No implication as to precisely when the Ca^{2+} binds to the protein is intended by the portion of this scheme on the right. The squares represent subunits in a state which does not allow rapid exchange of water with bound Mn^{2+}. We suggest that the rate-determining step of the Mn^{2+} binding process in the presence of Ca^{2+} is the association of the second Mn^{2+} to the Con A dimer. A fast change in conformation following this association results in the removal of Mn^{2+} from water exchange. The rate of this conformational change may be the rate of the process observed in PRR time courses upon addition of Ca^{2+} to Con A preincubated with Mn^{2+} (Figure 4). Indeed this process is faster than the binding of the second Mn^{2+} to the Con A dimer (Figures 1 and 4). It is clear that the mechanism of Mn^{2+} binding in the absence of Ca^{2+} (the left side in Figure 9) is different from that in the presence of Ca^{2+}. In the absence of Ca^{2+}, Mn^{2+} binds rapidly to noninteracting sites (Alter et al., 1977). For this reason the subunits not preincubated with Ca^{2+} are represented by triangles and hexagons rather than circles.

The Ca^{2+} binding step in the proposed reaction scheme on the right in Figure 9 must occur prior to the binding of the second Mn^{2+} since in the absence of Ca^{2+} the binding characteristics of the second Mn^{2+} are different than in the presence of Ca^{2+}. Equilibrium measurements indicate Ca^{2+} binding to apo-Con A is pH dependent (Alter et al., 1977). Though it binds to apo-Con A with reasonable affinity near pH 7.0, at lower pH values, where Ca^{2+} binding is weak, Ca^{2+} causes dramatic changes in the kinetic and equilibrium behavior for the binding of the second Mn^{2+}. Equilibrium binding studies demonstrate that Ca^{2+} binding in the pH range 5.0–7.0 is enhanced by prior association of Mn^{2+} (Kalb & Levitzki, 1968; Alter, 1975). Under these conditions the affinity of Ca^{2+} for Con A with bound Mn^{2+} is substantial even at low pH. Ca^{2+} binding to site S2, therefore, may occur after association of the first Mn^{2+} to a Con A dimer but before the association of the second Mn^{2+}. Because the stoichiometry of Ca^{2+} binding has not yet been established and heterogeneity in the Ca^{2+} binding is indicated (Kalb & Levitski, 1968; Alter et al., 1977), association of additional Ca^{2+} ions may occur later in the reaction scheme summarized on the right in Figure 9.

Alternate reaction sequences may exist and cannot be ruled out. For example, the rate-limiting step could occur following association of a second Mn^{2+} to the Con A_2–Mn complex. For this process to be consistent with the kinetic data, the affinity of all second Mn^{2+} sites on a Con A dimer must be very low until a rate-determining conformational change occurs. If the affinity were relatively high, the association rate observed in ESR spectroscopy would be faster than the rate observed in the PRR measurements as most of the Mn^{2+} would be bound before the rate-limiting step observed in the PRR studies occurs.

Brown et al. (1977) recently examined the kinetics of metal ion addition for the pathway in our model (Figure 9) which goes from triangles to hexagons to squares. This is also the pathway examined by Grimaldi & Sykes (1975). We have examined the alternate route. Brown & co-workers (1977) followed proton relaxivity changes following addition of Mn^{2+} to demetallized Con A or addition of Ca^{2+} to Con A treated with Mn^{2+}. For the latter experiment, increasing the Ca^{2+} concentration increased the rate of observed relaxivity changes. In our analogous experiment we obtained similar results. Ca^{2+}, when added in large excess, leads to the rapid change in ϵ^* shown in Figure 4. Our activation energies at pH 5.1 are similar to the 21.7 kcal calculated by Brown & co-workers (1977). They attribute the process measured to a conformational change from an unlocked to a locked form. In our experiments the binding of Mn^{2+} was followed directly by ESR spectroscopy. If the conformational change occurred slowly following that step, the PRR studies should have given a different rate law with different activation parameters, unless the second Mn^{2+} binding site per Con A dimer has very low affinity prior to the conformational change. Presently the most direct interpretation of our results is that Mn^{2+} association in the presence of Ca^{2+} is the rate-limiting step. The exact role of Ca^{2+} in influencing the Mn^{2+} association rate and cooperative binding in the Con A dimer is not now known and is the subject of future work.

Both the temperature dependence of the rate processes and their pH dependences suggest details of the rate-limiting step. Activation parameters obtained on both the high and the low pH side of the rate maximum suggest what types of interactions may be involved in the rate-limiting step. The activation enthalpies at pH 5.1 are quite consistent, with the binding of Mn^{2+} favoring deprotonation of one or more ionizable groups (Kauzmann, 1959; Edsall & Wyman, 1958). These are partially or totally unprotonated at pH 6.45 resulting in a reduced activation enthalpy at that pH. The large entropies which are observed at both pH values could arise from dehydration of a portion of the protein molecule, from a reordering of its structure, or from both processes. The extent of reordering or dehydration which is required in the rate-determining step, however, must be less at the higher pH. The

pH profiles of the rate constants suggest which ionizable groups affect the rate process. Two groups with pK values similar to histidine are implicated. Ca^{2+} must also affect the ionization of these groups since the pH–rate profiles for Mn^{2+} association depend on Ca^{2+}. Ca^{2+} concentrations used in this study were chosen to produce a maximum effect. The details involving Ca^{2+} influence on pH profiles of rate constants at lower Ca^{2+} concentrations are currently being studied in our laboratory.

Interactions between the various ligand binding sites on Con A are reflected by the reduction in Mn^{2+} dissociation rates when Ca^{2+} or Ca^{2+} and methyl α-D-mannoside are present. This reduction is consistent with other observations. Ca^{2+} both increases the affinity for the second Mn^{2+} on a Con A dimer and decreases the rate of Mn^{2+} association. A reduced dissociation rate is the expected consequence. Further reduction in the dissociation rate in the presence of sugar suggests that sugar stabilizes the protein conformation. Our results are in good agreement with the prediction of Hardman & Ainsworth (1976) that bound saccharides should reduce the rate of dissociation by Mn^{2+} from Con A.

In view of the reported crystal structure for Con A, it is interesting to speculate on the structural components of the protein which may contribute to its binding behavior. Crystal structure data (Hardman & Ainsworth, 1972; Becker et al., 1975) suggest that His-24 and several carboxylate residues are involved directly in Mn^{2+} binding. One of the carboxylates, Asp-19, is part of a polypeptide loop of residues 12–22. This loop, though part of the Mn^{2+} and Ca^{2+} binding site, might be mobile since it is located on the protein surface. Barber & Carver (1973) indeed have suggested that this loop is mobile and may be involved in time-dependent changes in proton relaxation enhancement. Following their suggestion, it is possible that carboxyl residues Asp-16 and Asp-19 of this mobile loop interact with His-205 located near the binding area (Hardman & Ainsworth, 1972; Edelman et al., 1972; Becker et al., 1975) and leave the metal binding region open to solvent. The pK values we observe may reflect protonation of His-24 or of His-205. At present, we cannot unequivocally present a mechanism to explain the pH optimum. One suggestion, however, is that the higher pK may represent titration of His-205. At high pH, the loop may close over the metal ion site, even when Mn^{2+} is not bound. Upon lowering the pH, His-205 becomes protonated, the loop folds back from the metal binding region to hydrogen bond to protonated His-205, and the site opens for Mn^{2+} entry. Upon protonation of His-24, this Mn^{2+} ligand can no longer bind its metal ion. Protonation of His-24 could then give rise to the lower pK observed. Activation parameters are consistent with this model since the activation enthalpy at pH 5.1 would result, at least in part, from the ionization of His-24 and of His-205. The latter residue could be involved in an electrostatic interaction with carboxylates of the surface loop. These ionizations are characterized by enthalpies of about 7 kcal/mol (Kauzmann, 1959; Edsall & Wyman, 1958). At pH 6.45 the activation enthalpy involving either His-205 or His-24 or both would be considerably less since both histidines may not be protonated. The approximately 14-kcal difference in activation enthalpy between pH 5.1 and 6.45 (Table I) agrees well with this model. The activation entropy reasonably results from either dehydration at the metal binding site as the loop covers the bound Mn^{2+} or a loosening of the loop structure. Using this model, we suggest that at pH 6.45 the loop would be in a partially closed position so that the metal binding site is at least partially dehydrated. The dehydration of the binding area coincident with binding at this pH would be expected to be less extensive than at pH 5.1. Additionally, at pH 6.45 the loop might lose mobility as it closes on the metals, causing a negative contribution to the activation entropy. In contrast, at pH 5.1 the open loop may be more rigid than at pH 6.45, since it could be hydrogen bonded to His-205. The mobility of the loop may not change appreciably upon binding the metal at pH 5.1 and, therefore, not produce as great a negative contribution to the activation entropy at pH 6.45 as at pH 5.1. This is consistent with the proposed model. Finally, slow dissociation of Mn^{2+} from the Mn–Ca–Con A and the methyl α-D-mannoside–Mn–Ca–Con A complexes (Figure 8) is consistent with Ca^{2+} and methyl α-D-mannoside's both favoring closure of the polypeptide loop around the metal binding sites. Presumably this loop would have to open for Mn^{2+} to dissociate from its binding site, and this could be a very slow process in the presence of Ca^{2+} or Ca^{2+} and a saccharide.

Since deprotonation of both histidine residues leads to the proper positioning and ionization state of ligands directly involved in metal binding, this model is in agreement with the uniform increase in Mn^{2+} binding affinity which accompanies increasing pH (Alter et al., 1977). A possible structural basis for the cooperativity in Mn^{2+} binding which is induced by Ca^{2+} is not now apparent. It must, however, involve a series of interactions which connect metal binding sites on the dimer which are 30–40 Å apart.

References

Abe, Y., Iwabuchi, M., & Ishii, S. (1971) *Biochem. Biophys. Res. Commun. 45*, 1271.

Agrawal, B. B. L., & Goldstein, I. J. (1967) *Biochim. Biophys. Acta 147*, 262.

Alter, G. M. (1975) Ph.D. Thesis, Washington State University, Pullman, WA.

Alter, G. M., Pandolfino, E. R., Christie, D. J., & Magnuson, J. A. (1977) *Biochemistry 16*, 4034.

Barber, B. H., & Carver, J. P. (1973) *J. Biol. Chem. 248*, 3353.

Barber, B. H., & Carver, J. P. (1975) *Can. J. Biochem. 53*, 371.

Becker, J. W., Reeke, G. N., Wang, J. C., Cunningham, B. A., & Edelman, G. M. (1975) *J. Biol. Chem. 250*, 1513.

Bittiger, H., & Schnebli, H. P., Eds. (1976) *Concanavalin A as a Tool*, Wiley, New York, NY.

Brown, R. D., Brewer, C. F., & Koenig, S. H. (1977) *Biochemistry 16*, 3883.

Connick, R. E., & Fiat, D. (1966) *J. Chem. Phys. 44*, 4103.

Dwek, R. A. (1973) *Nuclear Magnetic Resonance in Biochemistry*, p 247, Oxford University Press, London.

Dye, J. L., & Nicely, V. A. (1971) *J. Chem. Educ. 48*, 443.

Edelman, G. M., Cunningham, B. A., Reeke, G. N., Becker, J. W., Waxdal, M. J., & Wang, J. L. (1972) *Proc. Natl. Acad. Sci. U.S.A. 69*, 2580.

Edsall, J. T., & Wyman, J. (1958) *Biophysical Chemistry*, p 464, Academic Press, New York, NY.

Goldstein, I. J., Hollerman, C. E., & Smith, E. E. (1965) *Biochemistry, 4*, 876.

Goldstein, I. J., Reichert, C. M., Misaki, A., & Gorin, P. A. J. (1973) *Biochim. Biophys. Acta 317*, 500.

Grimaldi, J. J., & Sykes, B. D. (1975) *J. Biol. Chem. 250*, 1618.

Hardman, K. D., & Ainsworth, C. F. (1972) *Biochemistry 11*, 4910.

Hardman, K. D., & Ainsworth, C. F. (1976) *Biochemistry 15*, 1120.

Kalb, A. J., & Levitski, H. (1968) *Biochem. J. 109*, 669.

Kauzmann, W. (1959) *Adv. Protein Chem. 14*, 1.
Koenig, S. H., Brown, R. D., & Brewer, C. F. (1973) *Proc. Natl. Acad. Sci. U.S.A. 70*, 475.
Laidler, K. J. (1965) *Chemical Kinetics*, pp 15-17, McGraw-Hill, New York, NY.
Lis, H., & Sharon, N. (1973) *Annu. Rev. Biochem. 42*, 541.
Meirovitch, E., Lutz, Z., & Kalb, A. J. (1974) *J. Am. Chem. Soc. 96*, 7542.
Nicolau, C., Kalb, A. J., & Yariv, J. (1969) *Biochim. Biophys. Acta 194*, 71.
Poretz, R. D. (1968) Ph.D. Thesis, State University of New York at Buffalo, Buffalo, NY.
Reed, G. H., & Cohn, M. (1970) *J. Biol. Chem. 245*, 662.
Shephard, G. R., & Gurley, L. R. (1966) *Anal. Biochem. 14*, 356.
Shoham, M., Kalb, A. J., & Pecht, I. (1973) *Biochemistry 12*, 1914.
von Goldhammer, E., & Zorn, H. (1974) *Eur. J. Biochem. 44*, 195.
Wang, J. C., Cunningham, B. A., & Edelman, G. M. (1971) *Proc. Natl. Acad. Sci. U.S.A. 68*, 1130.
Weber, K., & Osborn, M. (1969) *J. Biol. Chem. 244*, 4406.
Yariv, J., Kalb, A. J., & Levitzki, A. (1968) *Biochim. Biophys. Acta 165*, 303.

Temperature-Dependent Spin Equilibrium of Microsomal and Solubilized Cytochrome P-450 from Rat Liver†

Dominick L. Cinti,* Stephen G. Sligar, G. Gordon Gibson, and John B. Schenkman

ABSTRACT: In the absence of exogenous substrate, temperature-induced type I and reverse type I (formerly called modified type II) spectral changes were observed with both rat liver microsomes and solubilized, partially purified cytochrome P-450. Similar changes were observed in the absolute spectrum of cytochrome P-450, i.e., increasing temperature reduced the absorption peak at 418 nm while simultaneously enhancing absorption in the 370–390-nm region in both liver preparations. An isosbestic point at 407 nm was noted and is indicative of a two-state equilibrium system. Spectral titration of type I and reverse type I spectral changes at 385 and 419 nm by dual wavelength spectrophotometry resulted in a slightly sigmoid-shaped curve with changes in temperature (3–40 °C). A graph of the log of the equilibrium constant vs. reciprocal temperature yielded a linear van't Hoff plot. From the slope and intercept an overall enthalpy change, $\Delta H = -14.66$ kcal/mol, and entropy change, $\Delta S = -49.88$ eu, in the reaction P-450$_{LS}$ ↔ P-450$_{HS}$ were obtained for hepatic microsomes. These thermodynamic parameters yield an equilibrium constant of 0.930 at 20 °C, indicating a significantly large amount (>48%) of high-spin cytochrome P-450 in the absence of added substrate, as corroborated by electron paramagnetic resonance spectroscopy. In contrast, the soluble cytochrome P-450 preparation yielded $\Delta H = -5.5$ kcal/mol and $\Delta S = -14.1$ eu. These state functions produced an equilibrium constant of 0.096 at 20 °C indicative of P-450 predominantly in the low-spin ferric form. These differences suggest that the microsomal environment of lipid and/or endogenous substrate has a dramatic effect on controlling the spin equilibrium. In addition to these thermodynamic parameters, the precise absolute extinction coefficients for pure high-spin and pure low-spin cytochrome were derived. These parameters for solubilized P-450 of $\epsilon_{HS} = 52$ mM^{-1} cm^{-1} and $\epsilon_{LS} = 126$ mM^{-1} cm^{-1} at 418 nm and the corresponding values for the membrane-bound protein indicate that only 54% of microsomal P-450 undergoes a temperature-dependent spin transition. For the liver microsomes, $\Delta\epsilon_{385-419nm}$ was found to be 126 mM^{-1} cm^{-1}.

Narasimhulu et al. (1965) observed the formation of a spectral transition in the Soret region of cytochrome P-450 upon addition of a steroid to a suspension of adrenal cortical microsomes. Less than 1 year later, two types of spectral changes were described when various drugs were added to liver microsomes (Remmer et al., 1966; Schenkman et al., 1967; Imai & Sato, 1966). One spectral change, termed "type I", was characterized by an absorption maximum at 385–390 nm and a minimum at 420 nm; a second spectral change, called "type II", was shown to possess absorption maxima at 425–435 nm and minima at 390–400 nm (Schenkman et al., 1967). A third spectral transition, initially called "modified type II", displayed an essentially mirror image of the type I spectral change and was subsequently described as a "reverse type I" spectral change (Schenkman et al., 1973). All three spectral transitions are induced following substrate addition to a liver microsomal suspension.

Mason and co-workers (1965a,b) described an electron paramagnetic resonance (EPR) spectrum in liver microsomes which resembled low-spin ferrihemoproteins and suggested that the EPR signal was related to cytochrome P-450. Cammer et al. (1966) reported similar findings and in addition showed that both type I and type II substrates affected the low-spin g_x and g_z components of the first-derivative EPR spectrum in opposite directions. For example, in the presence of aniline (type II substrate), the g_x signal was shifted to higher field while the g_z signal was shifted to lower field; the opposite occurred in the presence of hexobarbital, a type I substrate (Cammer et al., 1966). A conversion of the low-spin ferric hemoprotein to the high-spin form following addition of camphor was reported in the *Pseudomonas putida* cytochrome P-450 system by Tsai et al. (1970) and Peterson (1971). The spin state of ferric cytochrome P-450 can thus be modulated by substrate addition, shifting from low to high spin with type I compounds, vice versa with reverse type I compounds, or forming a new low-spin species with type II compounds. Similar spin-state changes occurred with adrenal cortex

† From the Department of Pharmacology (D.L.C., G.G.G., and J.B.S.), University of Connecticut Health Center, Farmington, Connecticut 06032, and the Departments of Molecular Biophysics and Biochemistry (S.G.S.), Yale University School of Medicine, New Haven, Connecticut 06510. *Received June 28, 1978.* This study was supported in part by U.S. Public Health Service Grants GM17021, GM24976, and RR07015 and a grant from the University of Connecticut Research Foundation.

0006-2960/79/0418-0036$01.00/0